Seventh International Conference on Computational Fluid Dynamics (ICCFD7), Big Island, Hawaii, July 9-13, 2012

ICCFD7-1905

Wavelet decomposition of turbulent velocity and its application to subgrid scale modeling

J.A. Denev*, C.J. Falconi* and H. Bockhorn*
Corresponding author: jordan.denev@kit.edu

* Karlsruhe Institute of Technology, Germany

Abstract: The paper presents results from Large Eddy Simulations of the flow in the TECFLAM (TYPE II) combustion configuration which by its complexity is a severe test for numerical simulations. A novel subgrid-scale model (called WALES: Wavelet Adapted Large Eddy Simulation) developed and presented earlier [1, 2] is verified with available experimental data and shows good agreement. Results with the Smagorinsky model are presented as well for comparison. The WALES model which, unlike the Smagorinsky model, distinguishes between laminar and turbulent flow regions, was applied without special near-wall treatment; despite this both models show close results. The investigation was carried out on a parallel supercomputer using 120 processors and Message Passing Interface (MPI).

Keywords: Wavelet Decomposition, Wavelet Adapted Large Eddy Simulation, Turbulence Modeling, Combustion Chamber Flow

1 Introduction

The present investigation aims at the application and verification of newly developed subgrid-scale models in the framework of Large Eddy Simulations (LES). Based on Direct Numerical Simulations (DNS) of a round jet in crossflow, presented in earlier works of the authors [3, 4, 5], and on the subsequent analysis of the results obtained, new modelling approaches [1, 2] within research programs of the German Research Association (DFG) have been developed. The novel approach consists in embedding wavelet decomposition into the subgrid-scale modelling within LES. New possibilities arise by this methodology as wavelets can distinguish between laminar and turbulent regions of the flow as well as to identify signal irregularities due to coherent structures in the flow.

The TECFLAM configuration, consisting of an axisymmetrical swirl burner and a cylindrical combustion chamber, is a suitable test for the developed new wavelet-based models: detailed experimental data obtained with LDA in the cold regime exist [6]. At the same time the TECFLAM configuration possesses several features, which make it difficult to simulate and model:

- small size openings coexist with a very large chamber dimensions which requires a large number of grid points
- largest velocities appear at the exit of the annular swirler, where the computational cells need fine resolution thus causing very small time steps for the explicit time scheme utilized
- large recirculation areas of small velocities arise in the combustion chamber thus requiring large start-up and averaging times
- high swirl number flow challenges the accuracy of the subgrid-scale models

The above listed features raise the demand on High Performance Computing. The paper presents the basic feature of the wavelet-based subgrid-scale model and describes in great detail the required resources for the computations, closely related to the features of the engineering problem under consideration.

2 Geometry of the combustor, numerical grid and domain decomposition

The studied configuration (TECFLAM / TYPE II) consists of an annular swirling jet flowing into a combustor chamber. The swirl is created by a movable block generator, the vane angles of which can be altered in order to adjust the desired level of swirl. The TECFLAM configuration is experimentally investigated at the "Engler-Bunte-Institute" of the University of Karlsruhe and its description can be found in [6]. Its geometry is presented in Fig.1. The main dimensions are listed in Table 1.

A block-structured grid was used with 6.2 million hexahedral cells distributed in 620 numerical blocks. The numerical grid was created with the commercial software $ICEM-CFD\ Hexa$. It contains 96 grid cells in the azimuthal direction. With respect to the interdependencies of the O-grid presented in Fig.2 (top right) such a distribution results in a minimum radial spacing of $\Delta r = 0.6mm$ ($\Delta r/D_0 = 0.01$) near the jet outlet. The minimum axial spacing appears in the same area and is equal to $\Delta x = 0.5mm$ ($\Delta x/D_0 = 0.0083$). The radial spacing at the first cell near the wall of the chamber is $\Delta r = 1mm$ ($\Delta r/D_0 = 0.017$), while at the walls of the annulus it is $\Delta r = 0.5mm$ ($\Delta r/D_0 = 0.0083$). The stretching factor of the grid is less than 7% in all directions. The minimal angle for all cells in the domain is 45°. Some cross-sections of the three-dimensional grid are shown in Fig.2.

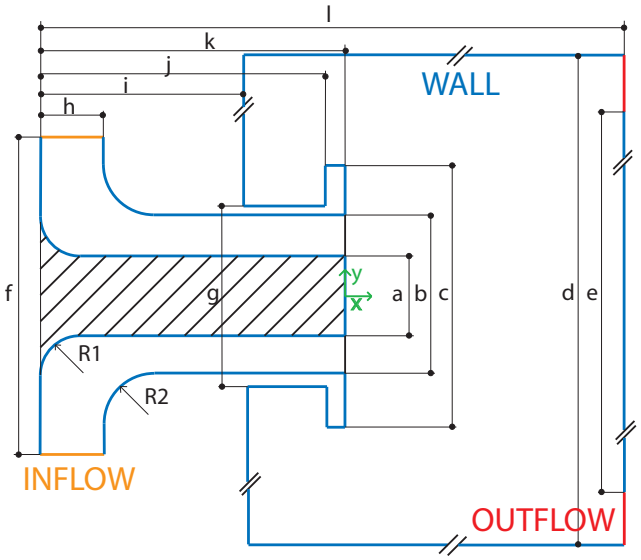

Figure 1: Geometry of the TECFLAM burner and the combustion chamber

Table 1: Dimensions of the TECFLAM configuration according to the drawing in Fig.1. All dimensions are given in $[mm]$. The characteristic length is the diameter of the annulus $D_0 = b = 60$ $[mm]$

a	b	c	d	e	f	g	h	i	j	k	l	R1	R2
30	60	100	500	460	120	70	24	77	107	114	1770	38	30

Results with the WALES model show that the near-wall resolution in wall units is the largest in the annular swirler near the jet outlet. At this location the grid nodes which are adjacent to the wall range $n_1^+ = 4 - 20$, where n_1^+ is the wall-normal distance. The lengths of the cells here is almost uniform in all three directions. At the walls of the combustion chamber the corresponding values are $n_1^+ = 4 - 8$.

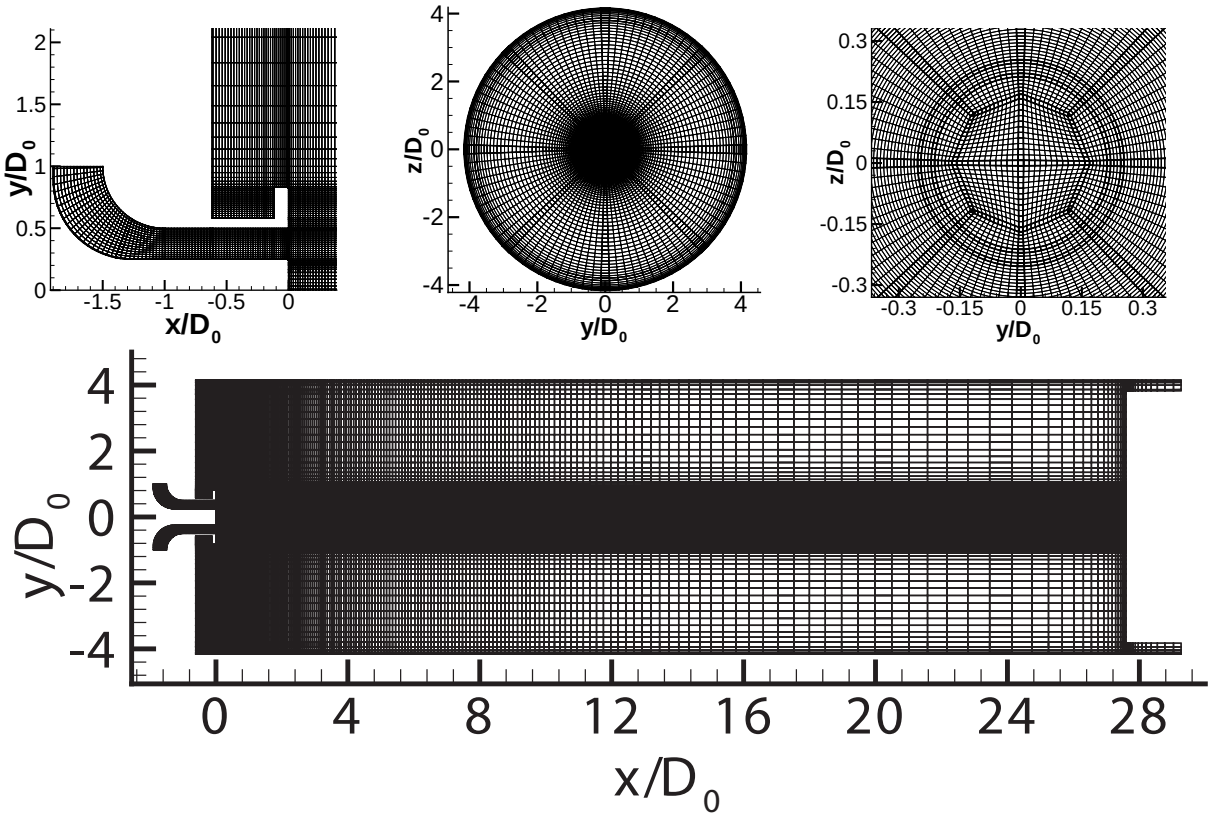

Figure 2: Computational grid for the TECFLAM burner. Top left: $y-x$ plane near the jet exit, every 2nd grid line is shown. Top middle: Cut in the $y-z$ plane of the entire computational domain. Top right: Zoom around the x-axis. Down: Overview covering entire domain at $z/D_0 = 0$, every 2nd grid line is shown.

3 Numerical method

The Navier-Stokes equations are discretized on a block-structured grid by means of the finite-volume method. The computations are carried out with an explicit Runge-Kutta time stepping and a pressure-correction equation. The method utilizes general curvilinear coordinates and is second-order accurate both in time and space. The parallelized numerical code LESOCC2 written in FORTRAN90 is used with MPI as a communication language. Further details of the numerical method and the code LESOCC2, developed at IfH of the University of Karlsruhe (TH), are presented by [7].

Recently, the original LESOCC2 code, specialized for Large Eddy Simulations, has been extended by the current WALES subgrid-scale model utilizing wavelet-details obtained from a biorthogonal wavelet decomposition. A short description of the WALES model is given below. Its basic idea and results are presented first in [1],[2]. Further applications of this model toward different flows can be found in [8].

The Smagorinsky model with a model constant equal to 0.1 is used in this paper for comparison.

4 Boundary conditions and flow parameters

No-slip boundary conditions are applied at all walls for the WALES computation, while wall functions of the Werner-Wengle type together with van Driest near-wall damping are used for the Smagorinsky model. A convective outflow condition is imposed at the exit of the computational domain. In order to resemble closely the experimental setup, this boundary condition is applied on a ring shape geometry ($\Delta x/D_0 = 1.67$)

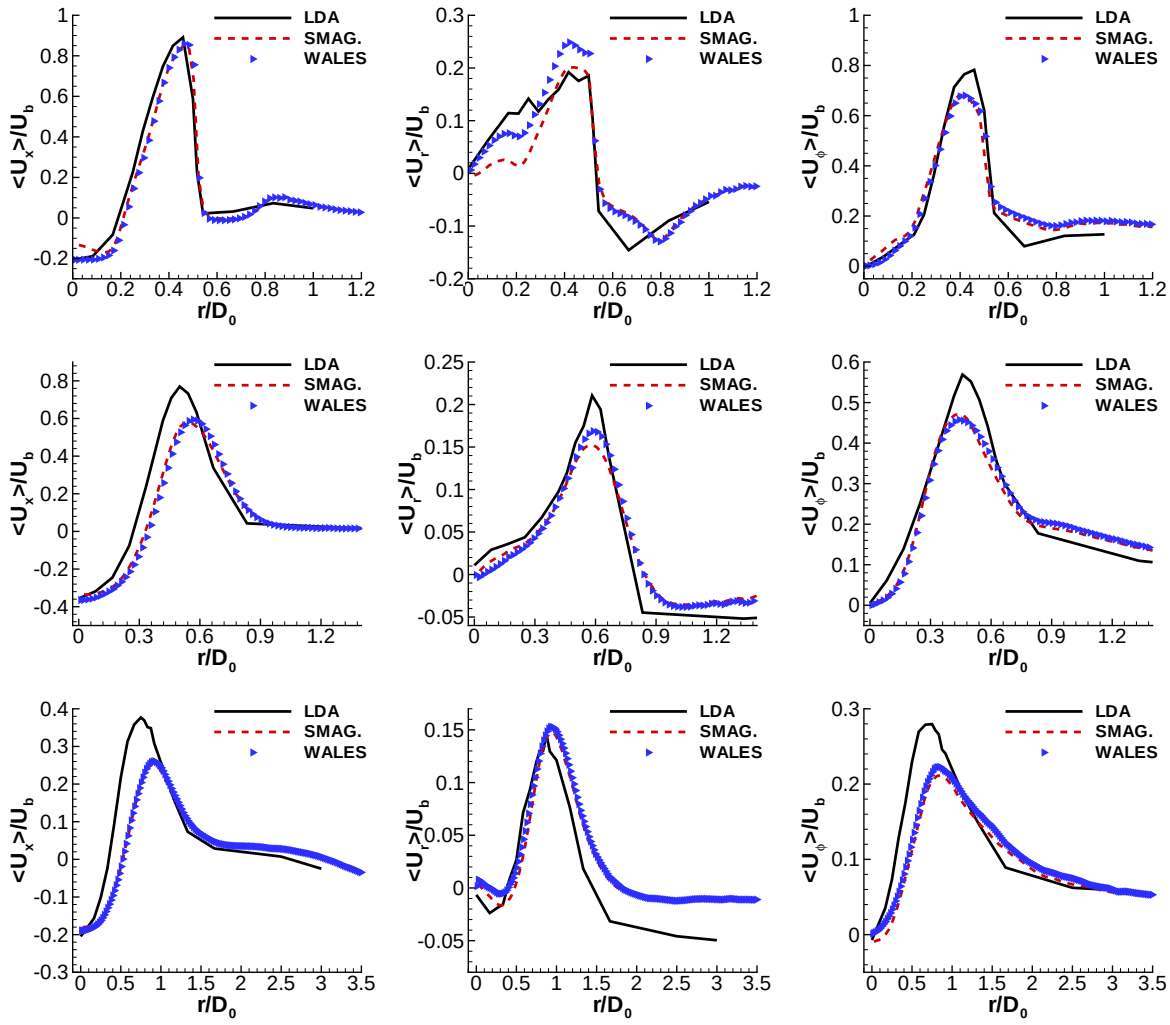

Figure 3: Results for the isothermal flow in the TECFLAM combustor. First row: Mean axial, radial and azimuthal velocity profiles, from left to right, at $x/D_0 = 0.0833$. Second row: Mean axial, radial and azimuthal velocity profiles, at $x/D_0 = 0.5$. Third row: Mean axial, radial and azimuthal velocity profiles, at $x/D_0 = 1.5$.

attached to the chamber as shown in Fig.2.

As the proper detailed representation of the swirl-generating device in the numerical grid is too demanding, instead, stationary block profiles are imposed for the radial as well as for the azimuthal velocity components at the circumferential inflow boundary (see Fig.1). Such a stationary approach to the swirling inflow condition was validated earlier in a similar combustor configuration studied in [9]. The applicability of this approach is confirmed by the good match of all quantities close to the jet exit with the experimental data in the present investigation. The explanation behind this is that turbulence readily develops in the annulus upstream of the exit of the jet issuing into the chamber.

The exact values for the velocity components at the inflow are $| < v > | = 6.174\ m/s$ for the radial velocity and $| < w > | = 11.84\ m/s$ for the azimuthal velocity. They result in a swirl number $S_0 = 0.9$. It is defined as the ratio of the angular momentum and the axial momentum multiplied with the outer radius

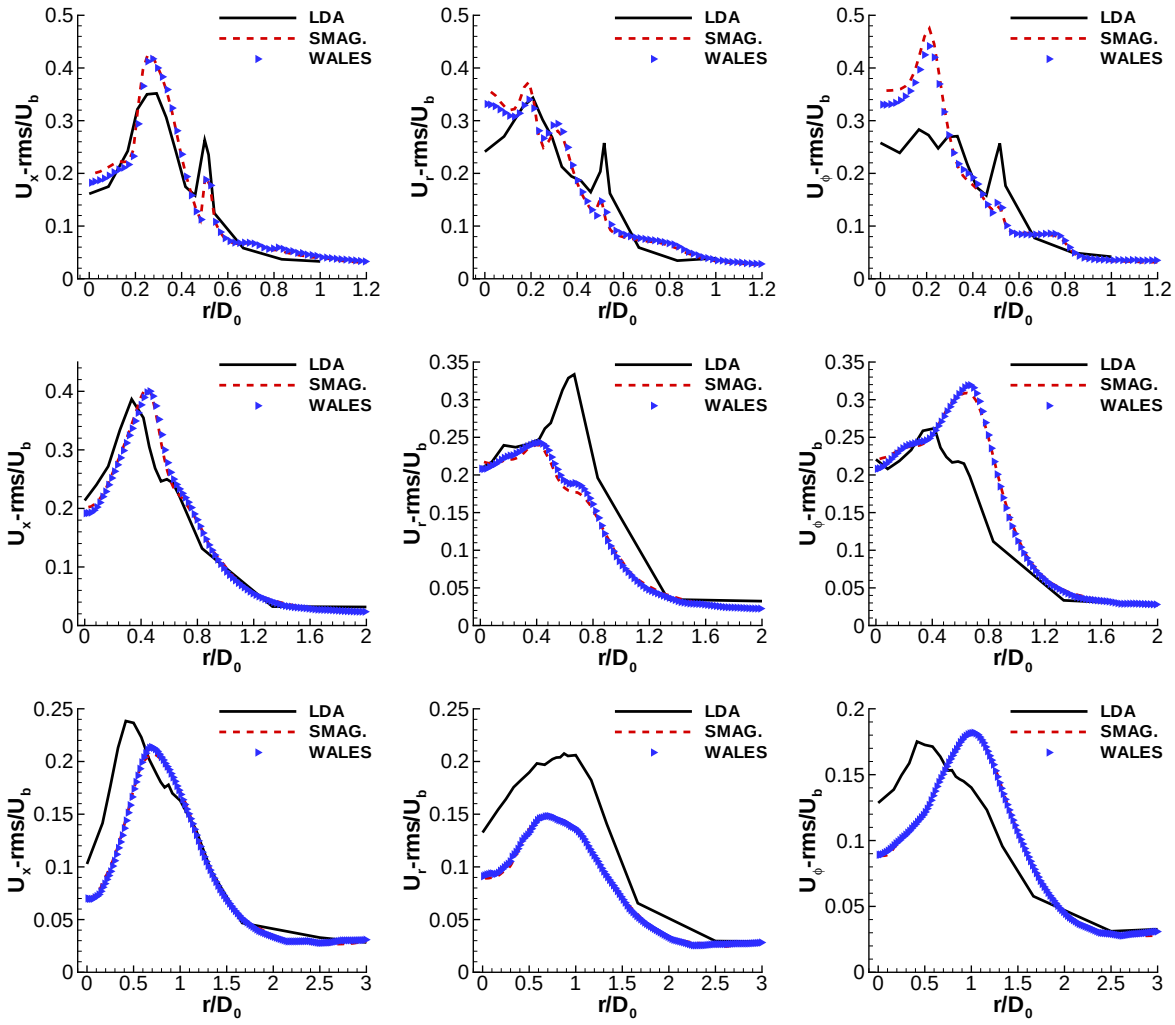

Figure 4: Results for the isothermal flow in the TECFLAM combustor. First row: Axial, radial and azimuthal velocity fluctuations profiles, from left to right, at $x/D_0 = 0.0833$. Second row: velocity fluctuations profiles at $x/D_0 = 0.5$. Third row: velocity fluctuations profiles at $x/D_0 = 1.5$.

$R_0 = D_0/2$ at the location where the jet issues into the combustion chamber:

$$S_0 = \frac{\int_0^{D_0/2} \rho\, u_x\, u_\phi\, r^2\, dr}{D_0/2 \int_0^{D_0/2} \rho\, u_x^2\, r\, dr}\,, \tag{1}$$

where u_x and u_ϕ are the axial and the azimuthal velocity components, respectively.

The inflow boundary conditions result in a mass flowrate of $m = 0.0664 kg/s$ which corresponds to the experimental data. The characteristic velocity $U_b = 39.51 m/s$ is calculated with this flowrate and the area of the annular cross-section which is equal to 0.009048 m^2. The Reynolds number which corresponds to this velocity and to the diameter $D_0 = 0.06m$ is equal to 159758. The same characteristic velocity and length are used for the estimation of the characteristic time t_0.

5 The WALES approach to subgrid-scale modelling

In the present section we describe the main features of our approach to subgrid-scale modelling named Wavelet-Adapted LES (WALES). This approach uses the biorthogonal wavelet decomposition of Harten [10] (see also [11]) to obtain the wavelet details. The wavelet decomposition is applied to the instantaneous velocity components (hereafter denoted as signals). The algorithm used in the present work is the following: first, based on a two-grid resolution (coarse- and fine-grid presentation of the signal), the wavelet-details for the signals are obtained. Then, based on the wavelet-details for each velocity component, the subgrid-scale turbulent viscosity is calculated using the following equation:

$$\nu_t = C_{WALES}(Vol_p)^{(1/3)}\sqrt{[detail(u)]^2 + [detail(v)]^2 + [detail(w)]^2}. \quad (2)$$

Here, C_{WALES} denotes a model constant which was set equal to 0.02 estimated from a calibration for turbulent channel flow. The quantity Vol_p is the volume of the computational cell on the finer grid, while $detail(u)$, $detail(v)$ and $detail(w)$ denote the wavelet details for the corresponding velocity component in the corresponding fine-grid cell.

Actually, there is no formal need to restrict the method to a two-level (two-grid) approach for the wavelet decomposition and hence involving more levels is also possible. However, the present two-level approach presents an optimum from a parallelization point of view: it requires the exchange of information from two neighbour cells across the block-boundary, which is synchronous with the need of the overall numerical method applied. Each additional wavelet-decomposition level would require additional exchange of information across the block boundary and would pose additional restrictions on the number of grid cells in each spatial direction (e.g. the grid points in each block should be an even number along each spatial direction for the present two-level approach; for three levels they should be a multiple of 4; for 4 levels - a multiple of 8 etc.).

Two main advantages result from the WALES approach. The first one stems from the features of the chosen wavelet decomposition (Hartens biorthogonal two-level decomposition) - a signal which is constant, linear or parabolic, simply results in zero wavelet details. As a consequence (and in contrast to the Smagorinsky model), laminar flows as such in e.g. long straight pipes, would automatically result in zero eddy-viscosity. The second advantage affects the algorithmic implementation of the WALES approach - tests in a straight periodic channel revealed that accurate results are obtained without special near-wall treatment. Thus, in the present investigation no wall-functions or wall-damping was applied.

6 Results and discussion

6.1 Computations - resources and averaging times

The computations were carried out using 120 processors of the parallel machine HP XC4000 at the High Performance Computing Center Stuttgart. For each of the two computations (denoted "WALES" and "Smagorinsky") the averaging time for obtaining the statistical quantities was 2180 t_0 which corresponds to $3.3s$ real (physical) time. The time for the simulations prior to start averaging was 2070 t_0 and 2200 t_0 for $WALES$ and $Smagorinsky$, respectively. The total wall-clock time for each computation was over 30 days (approx. 12 minutes wall-clock time for one dimensionless time unit t_0). The total number of time-steps for each computation is approx. 1.4 Mio. The two models require approx. the same CPU-time per iteration.

6.2 Verification with experimental data

Fig. 3 and 4 show the comparison of the calculations carried out with the WALES and the Smagorinsky models with available LDA measurements. Results are presented as radial profiles of the first and second moments of the velocity components close to the area where the air enters the combustion chamber (up to $x/D_0 = 1,5$). In this area the general agreement between experiments and both simulations is very good. In the zone where the annular jet enters the chamber ($x/D_0 = 0.083$) the simulations for both averaged- and rms-velocities match reasonably good the experimental values, thus indicating the correctness of the adopted stationary inflow conditions imposed at the circumferential inflow boundary.

The averaged velocities at ($x/D_0 = 0.083$) show the two typical shear layers (inner and outer) of the annular jet. The inner one ranges from $r/D_0 = 0.1$ to $r/D_0 = 0.46$ and the outer one - from $r/D_0 = 0.48$ to $r/D_0 = 0.6$. At larger r-values there is a change in the sign of the derivative for all three velocity components which stems from the recirculation zone behind the outer ring-like part of the combustor bluff body; this zone is shown further on in Fig.7. For the simulations this appears at approx. $r/D_0 = 0.8$, while in the measurements it differs for the different velocity components and ranges between ($r/D_0 = 0.66$ and $r/D_0 = 0.8$). Due to the small size of this recirculation zone (Fig.7) the change of sign of the derivative disappears downstream.

In the zone near the jet exit (up to $x/D_0 = 0.5$) the rms-values show two peaks which correspond to the inner and outer shear layers; the reader should note that they are not connected to the above discussed change in the sign of derivative of the averaged velocities at $r/D_0 > 0.8$. Such peaks are observed also by a different geometry (without the outer ring-like bluff body of the combustor), see e.g. [12]. The peaks in all velocity components disappear further downstream.

As a whole, the WALES model and the Smagorinsky model with the van Driest damping function and wall functions show generally a similar performance and results which are close to each other. Therefore, in the following, results obtained only with the WALES subgrid-scale model will be presented.

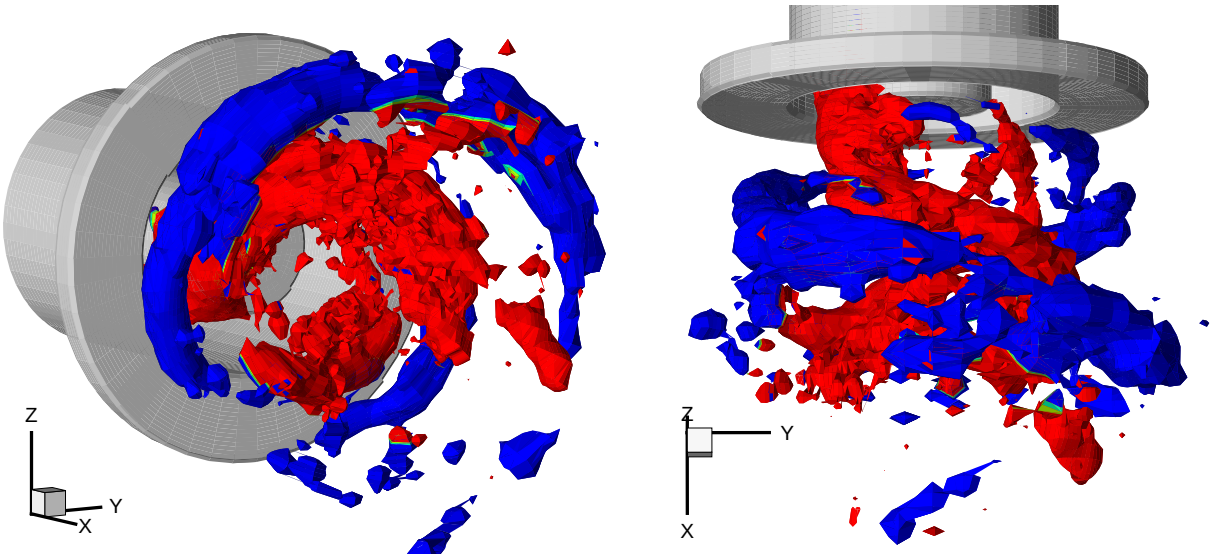

Figure 5: Visualization of large-scale coherent strcutures at the combustor exit. Isosurface of the pressure fluctuations $p' = (< p > -p)/(\rho U_b^2) = -0.1$. Isosurface color depends on the sign of the derivative $d < U_x > /dr$. Precessing vortex core: $d < U_x > /dr > 0$ (red). Outer stucture: $d < U_x > /dr < 0$ (blue).

6.3 Vortex structures

Two typical vortex structures as described e.g. in [13, 14] are presented in different colours in Fig. 5. They are attributed to the inner and outer shear layers of the annular jet, which have been discussed in the previous section. The method of identifying the vortex structures of the two shear layers is explaned in the text under the figure and is taken from [15]. As it can be seen in Fig. 5 the inner structures (called precessing vortex cores, PVC) are initially oriented along the downstream axis x after which they start to follow the swirl movement, while the outer structures appear oriented circumferentially immediately behind the exit of the annular jet.

This orientation delivers a reasonable explanation for the good correlation of the coherent vortical structures found in Fig.6 at $x/D_0 = 0.083$ (no outer structures are present at this distance). The correlation can be seen in the location of vortices identified by the instantaneous values for the pressure fluctuation (where vortex centers appear as minima) and the downstream velocity fluctuation (vortices here are identi-

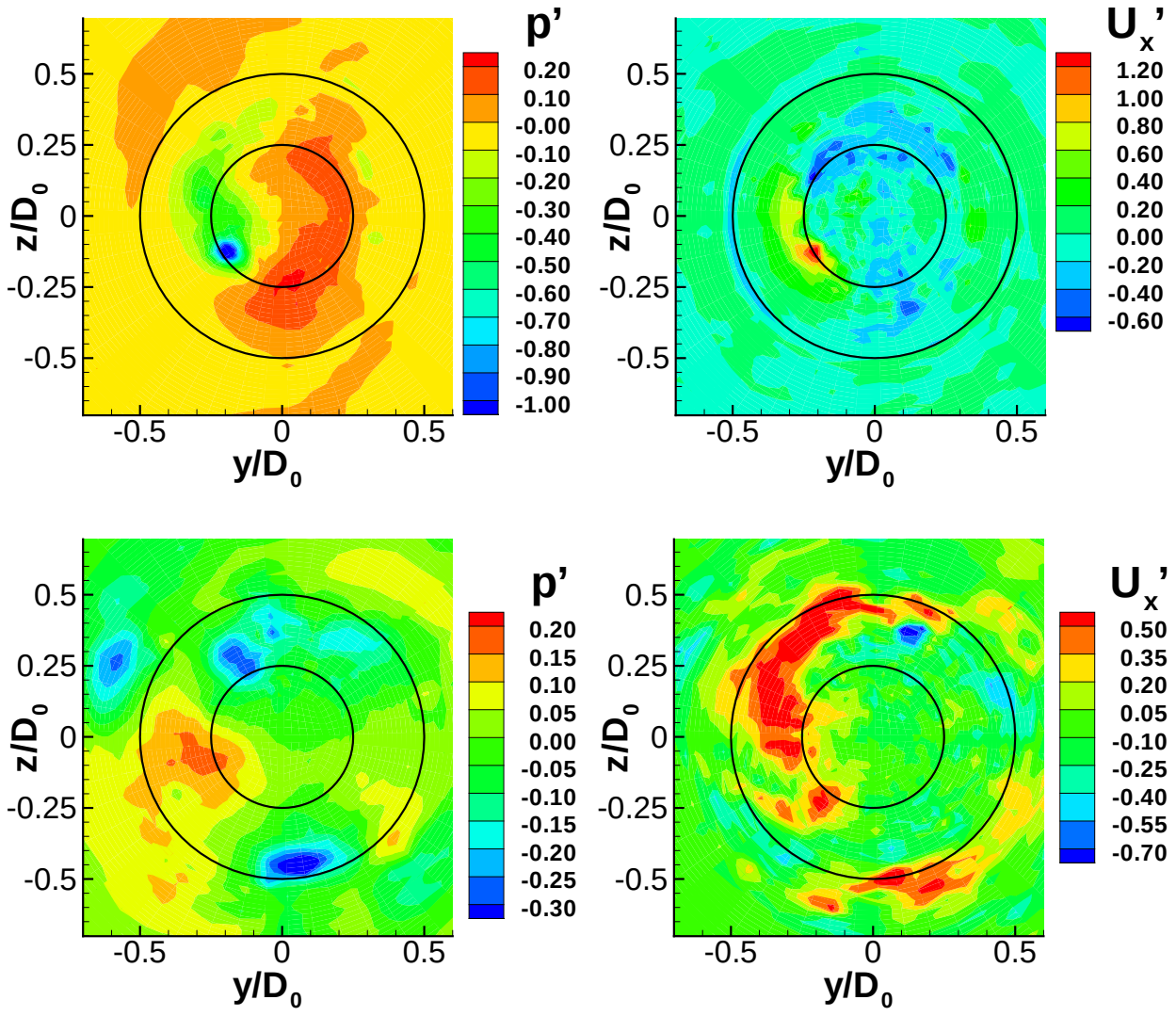

Figure 6: Countour plots of the pressure fluctuation $p' = (< p > -p)/(\rho U_b^2)$ and the axial velocity fluctuation $U_x' = (< U_x > /U_b) - (U_x/U_b)$, from left to right, at different x/D_0-planes. First row: $x/D_0 = 0.083$. Second row: $x/D_0 = 0.5$.

fied by corresponding maxima). However, with the change of orientation of the coherent structures further downstream (Fig.6 at $x/D_0 = 0.5$), this correlation appears to be not so pronounced. A good correlation at $x/D_0 = 0.5$ could also be not identified when comparing the corresponding plots for the fluctuations of U_r and U_ϕ with the pressure fluctuations (not shown).

Large recirculation zones of the averaged flow field are shown in Fig. 7 for the plane $y = 0$. The colours present the averaged kinetic energy of turbulence which has its maximal value close to the jet exit (behind the inner cylindrical bluff body of the combustor (lance)) and possesses large values downstream along the streamlines, thus indicating the position of the shear layers. It can be seen in the figure, that behind the cylindrical bluff body a recirculation zone is formed, which is known in the literature [12] as the geometry-induced recirculation zone (GRZ). Another zone, called central recirculation zone (CRZ) starts in the figure at $x/D_0 = 1.9$ and $y/D_0 = 0.7$ and is caused by the swirl flow. As shown in [12] it appears at sufficiently large swirl numbers and changes in shape and size with the change in the swirl number.

The TECFLAM configuration has an additional recirculation zone which is caused by the second, ring-shape bluff body (see Fig. 7) behind which a smaller GRZ is formed. The largest recirculation zone appears

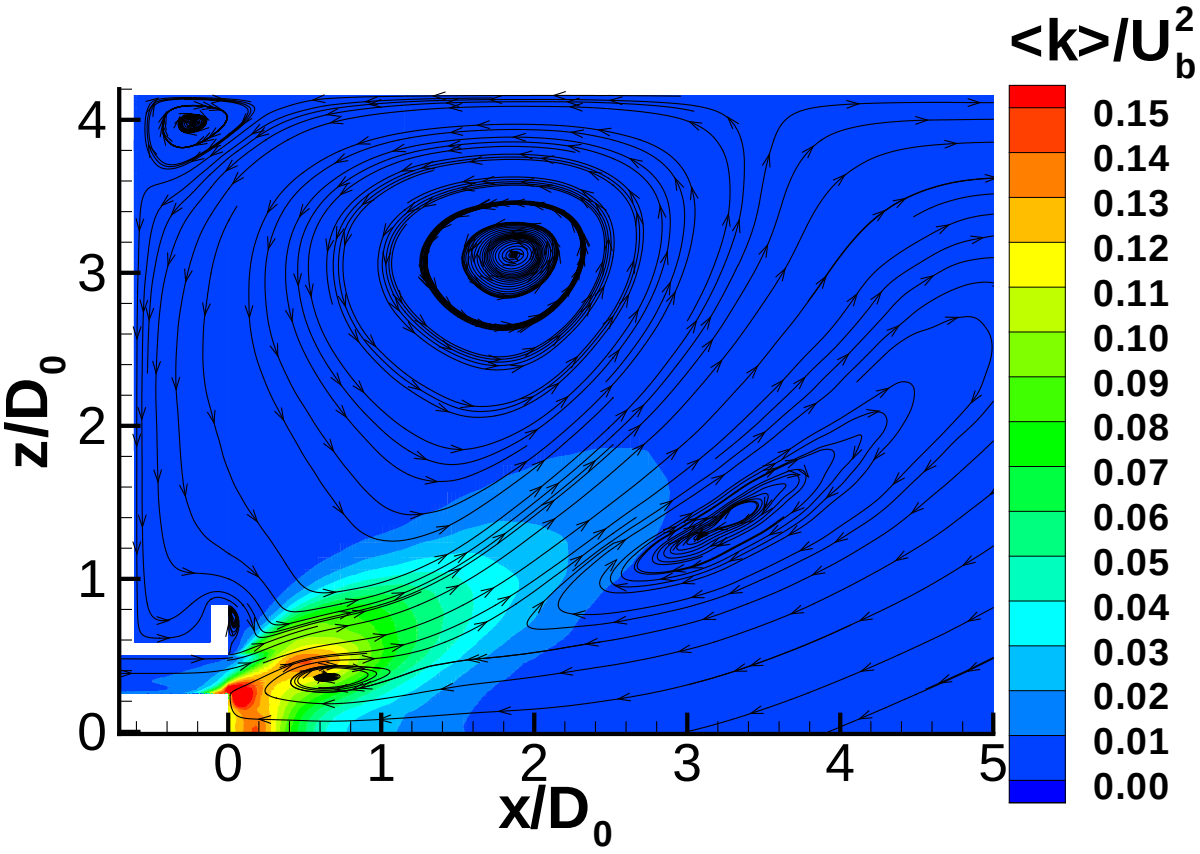

Figure 7: Countour plot of the kinetic energy of turbulence and 2d-streamlines of the average flow at the plane $y/D_0 = 0$.

between the jet shear layer and the wall. The velocities in this zone are relatively small, thus increasing enormously the required time for sampling of the statistics as well as the related computational resources. A smaller recirculation zone appears in the corner from the presence of the large recirculation zone.

7 Conclusions

The Large Eddy Simulation of the TECFLAM combustion configuration with a new subgrid-scale model has been presented. This present configuration (swirl number $S = 0.9$) presents a severe test for such numerical investigations thus requiring a very large amount of CPU-time. This required parallel computations on 120 processors of the HP XC4000 at the High Performance Computing Center Stuttgart (HLRS) to be carried out for a total duration of over one month wall-clock time.

The results with the new WALES subgrid-scale model, which uses a wavelet decomposition to obtain the eddy-viscosity, compare well to the experimental data available for the fluid flow in the combustion chamber. The WALES model gives results which are quite close to those of the Smagorinsky model, but without the need in near-wall modelling. It delivers zero eddy-viscosity in regions, where the signal is constant, linear, or parabolic (laminar flows).

Acknowledgements

The present project is funded through the DFG priority program SPP-1141 and a joint French-German CNRS-DFG Program on Computational Fluid Dynamics under the acronym FOR 507. The simulations were performed on the national super computer HP XC4000 at the High Performance Computing Center

Stuttgart (HLRS) under the grant with acronym "DNS-jet". The authors would like to thank to their colleagues Peter Habisreuther, Ilian Dinkov and Manuel García-Villalba for their valuable support.

References

[1] J. A.Denev, J. Fröhlich, C. J. Falconi, and H. Bockhorn. Direct numerical simulation, analysis and modelling of mixing processes in a round jet in crossflow. In H. Bockhorn et al., editor, *Springer series on Heat and Mass Transfer (Volume Title: Micro and Macro Mixing)*, pages 143–164. Springer Verlag Berlin Heidelberg, 2010.

[2] J. A. Denev, C. J. Falconi, J. Fröhlich, and H. Bockhorn. Wavelet-adapted sub-grid scale models for LES. In *Notes on Numerical Fluid Mechanics and Multidisciplinary Design*, volume 110/2010, pages 111–117. Spinger Verlag Berlin Heidelberg, 2009.

[3] J. A. Denev, J. Fröhlich, and H. Bockhorn. Direct numerical simulation of mixing and chemical reactions in a round jet into a crossflow. In W. E. Nagel, W. Jaeger, and M. Resch, editors, *High Performance Computing in Science and Engineering 06, Transactions of the High Performance Computing Center Stuttgart*, pages 237–251. Springer - Heidelberg - New York, 2006.

[4] J. A. Denev, J. Fröhlich, and H. Bockhorn. Direct numerical simulation of a round jet into a crossflow - analysis and required resources. In W. E. Nagel, D. Kroener, and M. Resch, editors, *High Performance Computing in Science and Engineering 07, Transactions of the High Performance Computing Center Stuttgart*, pages 339–350. Springer - Berlin - Heidelberg, 2007.

[5] J. A. Denev, C. Falconi, J. Fröhlich, and H. Bockhorn. DNS and LES of a jet in crossflow – Evaluation of turbulence quantities and modelling issues. In *Procs. of 7th Int. ERCOFTAC Symposium on Engineering Turbulence Modelling and Measurements, ETMM7*, volume 2, pages 587–592, Limassol, Cyprus, 4-6 June 2008.

[6] P. Schmittel, B. Günther, B. Lenze, W. Leuckel, and H. Bockhorn. Turbulent swirling flames: Experimental investigation of the flow field and formation of nitrogen oxide. *Symposium (International) on Combustion*, 28(1):303–309, 2000.

[7] C. Hinterberger. *Three-dimensional and depth-averaged Large-Eddy-Simulation of flat water flows.* PhD thesis, Inst. Hydromechanics, Univ. of Karlsruhe.

[8] H. Bockhorn, J. A. Denev, M. Domingues, C. J. Falconi, M. Farge, J. Fröhlich, S. Gomes, B. Kadoch, I. Molina, O. Roussel, and K. Schneider. Numerical simulation of turbulent flows in complex geometries using the coherent vortex simulation approach based on orthonormal wavelet decomposition. volume 104 of *Notes on Numerical Fluid Mechanics and Multidisciplinary Design (NNFM)*, pages 175–200. Springer Verlag Berlin Heidelberg, 2009.

[9] M. García-Villalba. *Large eddy simulation of turbulent swirling jets.* PhD thesis, Inst. Hydromechanics, 179p., ISBN 3-86644-015-4, Univ. of Karlsruhe, 2006.

[10] A. Harten. Discrete multi-resolution analysis and generalized wavelets. *J. Appl. Num. Math.*, 12:153–193, 1993.

[11] O. Roussel. *Development of an multiresolution adaptive three-dimensional algorithm for the solution of parabolic partial differential equations. Application to thermo-diffusive flame instabilities.* Phd thesis, University of Aix-Marseille II, France, 2003.

[12] M. García-Villalba and J. Fröhlich. Les of a free annular swirling jet – dependence of coherent structures on a pilot jet and the level of swirl. *Int. J. Heat Fluid Flow*, (27):911–923, 2006.

[13] A. K. Gupta, D. G. Lilley, and N. Syred. *Swirl Flows.* Abacus, London, 1984.

[14] C. M. Coats. Coherent structures in combustion. *Prog. Energy Combust. Sci.*, (22), 1996.

[15] M. García-Villalba, J. Fröhlich, and W. Rodi. Identification and analysis of coherent structures in the near field of a turbulent unconfined annular swirling jet using large eddy simulation. *Phys. Fluids*, 18:055103, 2006.